Enhancement Techniques to Design a Standalone PV System for Residential Application

R. Ramaprabha and S. Malathy

Abstract Standard design procedures are available to design a standalone solar photovoltaic (SSPV) system. However, it does not include the impact of partial shading on the PV array. The harvested power may reduce appreciably if the PV array is partly or completely shaded. The reduction is to be compensated by increasing the size of the PV array and this increases the overall cost of the system. It is therefore necessary to devise techniques to mitigate the impact of partial shading and enhance the power generation under such conditions. This chapter introduces and explains various strategies (shade resilient arrangement, global peak detecting algorithm, and reduced device count inverters) to incorporate along with the standard design procedures to increase the power generated by the SSPV system. Enhanced performance reduces the return on investment (ROI) period, thereby making the standalone PV system more attractive.

Keywords Photovoltaic · Partial shading · Shade tolerant configuration · GMPPT · Multilevel inverter

1 Introduction

The unrelenting focus among the countries on diversifying their energy mix away from imported oil and fossil fuels has widened the market for power generation using renewable energy sources. Power generation by photovoltaic (PV) systems has gained much attention than other renewable energy sources due to its abundant availability and nonpolluting nature. Further, the subsidies/incentives offered by the government and the technological advancements which have reduced the cost per watt have significantly increased the reach of PV technology among the general population.

R. Ramaprabha (✉) · S. Malathy
Sri Sivasubramaniya Nadar College of Engineering, Kalavakkam 603110, Tamil Nadu, India
e-mail: ramaprabhar@ssn.edu.in

S. Malathy
e-mail: smalathy@gmail.com

S. Motahhir and A. M. Eltamaly (eds.), *Advanced Technologies for Solar Photovoltaics Energy Systems*, Green Energy and Technology,
https://doi.org/10.1007/978-3-030-64565-6_10

The large-scale commercial installations are installed in shade-free areas. But, the small-scale residential SSPV systems are installed on the rooftops or facades of the buildings that are susceptible to shades due to space limitations. The shade is often caused by nearby buildings or structures in the same building.

Partial shading is a condition where all the panels in a PV array do not receive the same amount of irradiation. Clouds, bird litters, nearby buildings, or structures in the same building as chimneys and overhead tanks may cast their shade on the PV panels. When a PV array is shaded partially, the shaded panels generate lesser photon current and impose a current limitation on the other serially connected non-shaded panels. If this limitation is violated, the shaded panels get reverse biased, and hot spots may develop due to increased thermal stress. Bypass diodes prevent hot spot development by offering an alternate path for the current flow [1]. However, the shaded panel is completely bypassed and the residual power generated by the panel remains uncollected. The net power generated is significantly reduced under such circumstances and to meet the desired specifications, the size of the PV array is to be increased. This in turn increases the ROI that makes power generation by PV systems less attractive.

It is evident that partial shading is the major issue that needs to be addressed in an SSPV system. The simple solution is to provide bypass diodes to prevent the panels from getting damaged. However, the inclusion of bypass diodes causes multiple power peaks in the voltage-power characteristic curve, and to address this issue global maximum peak tracking (GMPPT) algorithms are to be included in the system. These algorithms track the global peak and make sure that maximum power is transferred from the array to the load under all environmental conditions. GMPPT algorithms based on soft computing techniques, artificial intelligence, and other search methodologies have been reported in the literature [2–5]. Some algorithms require advanced processors to do complex computations, while others require huge data set to train. The choice of the GMPPT algorithm relies on the user's requirements and availability of resources.

Further, the reduction in output power of partially shaded PV array is not directly proportional to the shade intensity but relies highly on the number and configuration of bypass diodes embedded in the panels, shade pattern and the interconnection scheme adopted in the array. The reduction in power is mainly due to mismatch in currents and it can be reduced to a greater extent by shade dispersion or irradiation equivalence [6]. Many schemes based on algorithms (online and offline) and puzzle patterns like Sudoku, magic square, and Latin square [7–9] have been proposed in the literature to equalize the irradiation. The underlying principle in all these strategies is to disperse the shade evenly all over the PV array to reduce the mismatch in currents among the serially connected panels. The online algorithms are dynamic and involve several sensors to assess the prevailing shading conditions [10–12]. The switches provided with each of the panels are then triggered appropriately to change the interconnectivity between the panels in the array. The offline algorithms are static and adopt puzzle patterns or thumb rules to fix the position of the individual panels in the array.

These two strategies (irradiation equivalence and global peak detecting) are discussed and analyzed separately by most of the researchers to address partial shading issues.

This chapter tends to unify these strategies into the standard design procedure to enhance the power generation under partially shaded conditions and to utilize the installed PV system efficiently.

The standard design procedure calculates the size of the array and the rating of other components to be included in the system. It does not take into account the impact of partial shading. The efficiency of the SSPV system can be enhanced appreciably if the irradiance equivalence algorithm is incorporated in the design stage to fix the location of panels within the array. One such strategy is discussed in Sect. 4. The irradiation cannot be equalized perfectly for all the shading conditions and in such cases; the electrical characteristics show multiple peaks. Several peak detecting algorithms are reported in the literature and two such algorithms are discussed in Sect. 5. The PV inverter failure rate is higher compared to the other components in the PV system and Sect. 6 discusses the strategy that can be adopted to improve the reliability. The design of an SSPV system for a residential unit is considered in this chapter to demonstrate the significance of improvisation strategies.

2 Standalone PV System

A standalone PV system has a PV array that is sized to meet the load requirements. The schematic of the typical SSPV system is depicted in Fig. 1.

The major components of the system include PV array, maximum power point tracking (MPPT) controller, battery bank, and inverter. The output power of the PV array is not constant and it depends greatly on the prevailing environmental

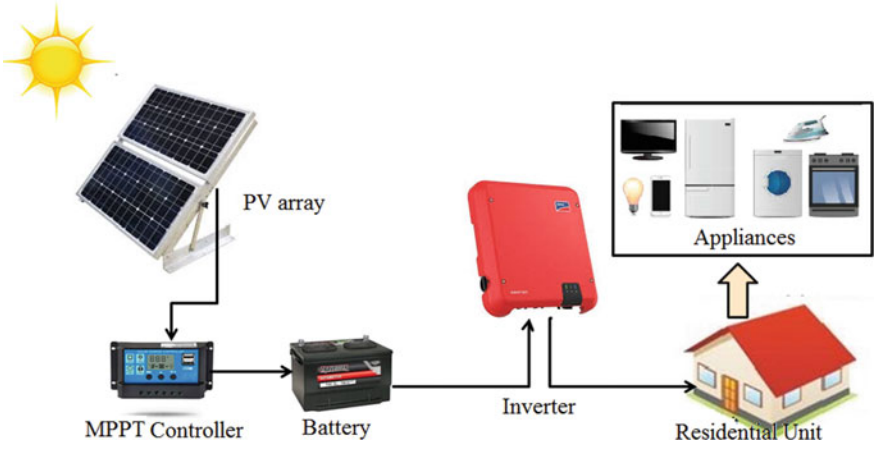

Fig. 1 Schematic of SSPV system

conditions. The MPPT controller operates the PV array at its optimal power point and ensures the transfer of maximum power from the source to the load under all environmental conditions. Most of the residential load operates on ac and hence an inverter is integrated into the standalone PV system. Commercial inverters have an inbuilt conventional MPPT controller. However, the conventional controller can't track the peak effectively under partially shaded conditions as it can't differentiate between global and local peaks, and consequently, the power extracted from the PV source is significantly less. The battery bank is essential in the SSPV system to enable the operation of the loads during night times. The battery bank size is determined considering the load requirements and days of autonomy.

Nowadays, batteryless systems are gaining popularity given the cost, size, and limited lifetime of the battery besides the impacts on the environment. Hence, in this work, the SSPV system that is directly connected to the residential load during the day (with a minimal battery bank to support short time mandatory loads) and connected to the grid during the night is considered.

As a design example, a residential unit located in Chennai, India is considered. The residential building is a single-family home with two floors and a built-up area of 1900 square feet. The photovoltaic power potential for the location is 4 kWh/kW_p (daily) and 1461 kWh/kW_p (yearly sum) [13] inclusive of the power conversion losses and losses due to dirt. Also, the power plant availability is assumed to be 100%. The design is given below.

- After efficiency improvements, the annual energy demand for the building is determined to be 12780 kWh/year. That is, E = 12780 kWh/year.

(Note: Energy demand can be calculated by considering either all possible loads of the residential building or the average annual energy consumed by the residential building from its electricity bill)

- Considering the solar energy resource for the location as 5.5 kWh/m^2/day, the average annual sunlight hours is calculated to be 2008 (5.5 × 365 = 2007.5) full sun hours.
- Required PV panel wattage rating = (12780 kWh/2008 h) = 6.365 kW.
- Considering 25% loss, PV Panel wattage = 6.365 kW/0.75 ≈ 8488 W.
- Considering 250 W_p panel with 31.5 V and 7.94 A at peak point, number of panels required = 8488/250 = 33.95 ≈ 35 panels.
- Number of panels in series = 7 (to meet the 220/230 V requirement).
- Number of strings in parallel = 5 (7 × 5 = 35).
- Voltage and current of 7 × 5 array are 220.5 V and 39.7 A (at max. power).
- Maximum power produced by 7 × 5 array ≈ 8750 W.

Appropriate power converter (power conditioning unit—PCU) can be introduced between the PV array and load to regulate voltage and current.

These calculations are done assuming standard test conditions (STC). But, the energy yield of the PV array may significantly fall if the array is shaded partially or completely. The PV array is usually installed on the rooftop (flat roof) and it is likely to be shaded partially by the parapet wall, overhead water tanks, antenna, cables, and

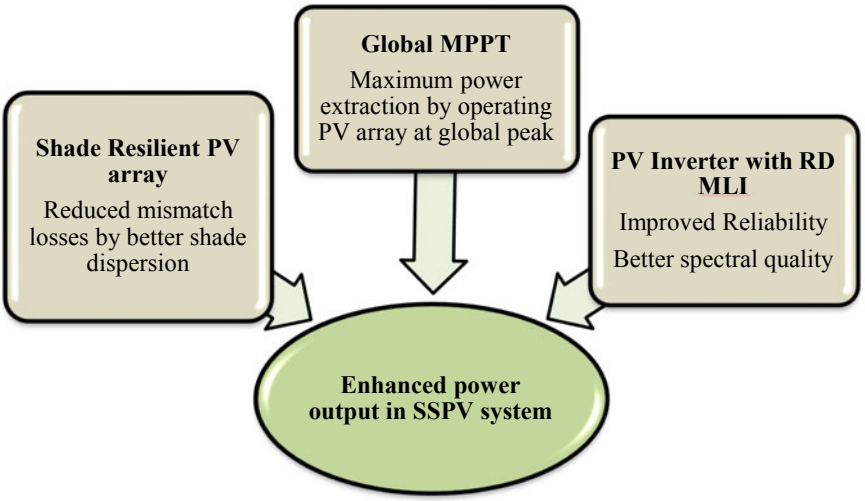

Fig. 2 Enhancement strategies for SSPV system

trees and nearby buildings beside the shading by bird litters and dirt accumulation. These shading conditions are caused by fixed objects/structures and hence can be categorized as fixed shadings.

Shading/partial shading is unavoidable and will prevail for a considerable duration in most of the urban residential installations. This results in reduced power generation and, to meet the load, the PV array is to be upsized and that is not a favorable option. This issue can be addressed by arranging the PV array in a shade resilient (SR) configuration where the shade tolerance of the PV array is enhanced by dispersing the shade uniformly all over the array. If the shaded geometry is short and narrow as in most of the cases, the voltage-power (V-P) characteristics of the SR PV array may exhibit multiple peaks, and incorporation of the global peak detecting algorithm will track and operate the PV array at its optimal power point. Further, the reliability of the SSPV system can be enhanced by employing a multilevel inverter with reduced device count (RD MLI) instead of the conventional inverter. The performance of the residential SSPV system can be enhanced with these three enhancement strategies (SR arrangement, GMPPT, and RD MLI). The enhancement strategies proposed in this chapter for the SSPV system are depicted in Fig. 2.

3 PV Array and Interconnection Schemes

The study considers a 7 × 5 array of 250 W_p panels. The mathematical model (single diode PV model) of the panel is developed based on the standard equations [14] to assess the power generation under partially shaded conditions. The specifications of

Table 1 Specifications of the 250 W_p PV Panel

Specifications	Values
Open circuit voltage (V_{oc})	37.8 V
Short circuit current (I_{sc})	8.7 A
Max. power (P_m)	250 W
Voltage at P_m (V_m)	31.5 V
Current at P_m (I_m)	7.94 A

the panel are presented in Table 1. The simulated electrical characteristics (voltage-power and voltage-current) of the 250 W_p panel are presented in Fig. 3. The peak or the maximum power is 250 W at standard conditions.

The peak power falls with irradiation as shown in Fig. 4. However, the voltage (V_m) at which the maximum power occurs varies slightly with irradiation. It is often neglected to ease calculations.

The panels in the PV array are connected in series and parallel to meet the voltage and current specifications. Series and parallel are the basic interconnection schemes and it has been proved in the literature that the parallel scheme results in optimal output under all environmental conditions [15]. However, higher array current and lower array voltage resulting from the parallel configuration are not desirable. Hence,

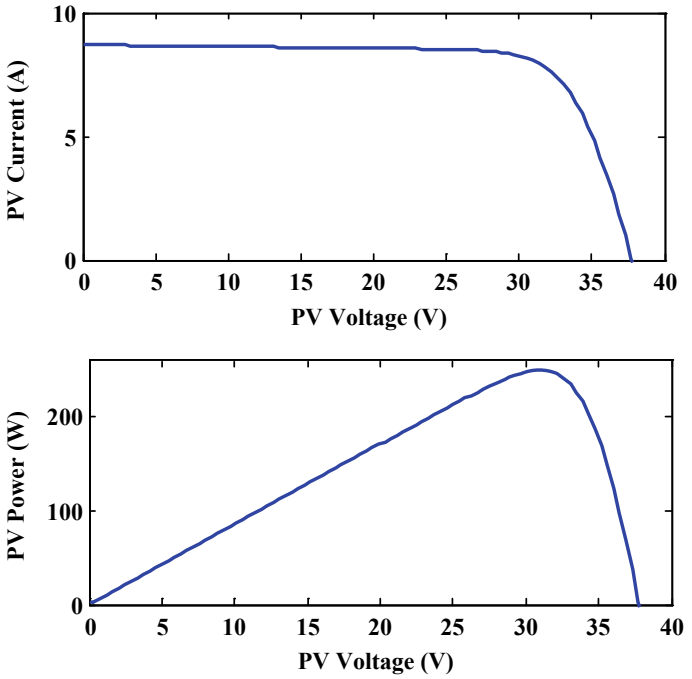

Fig. 3 Characteristics of 250 W_p panel

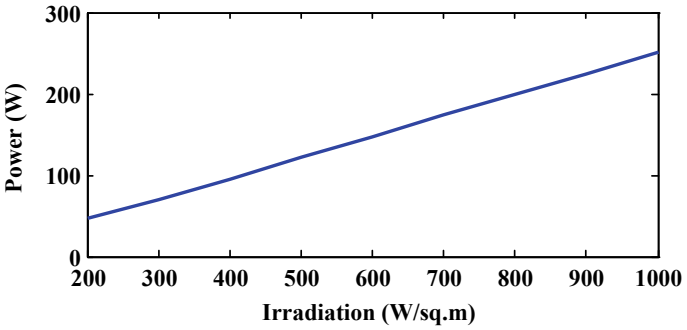

Fig. 4 Change in peak power (P_m) with irradiation

new interconnection schemes like the honey comb (HC), bridge link (BL), and total cross-tied (TCT) are derived from the basic schemes with the inclusion of cross-ties. The basic and derived interconnection schemes for the 7 × 5 PV array are presented in Fig. 5.

The simulated electrical characteristics of the 7 × 5 array for various interconnection schemes are presented in Fig. 6. The characteristics are simulated under standard test conditions. The series configuration results in a lesser array current at higher voltage levels. It is due to the fact that the array current is equal to the panel current in series connection. In the parallel configuration, the array current is equal to the sum of all the PV panel currents and this results in higher current at low voltage levels. In the case of the derived configurations, the array voltage depends on the number of panels connected in series, and the array current depends on the number of panels connected in parallel. The voltage and current levels of the array remain the same for the derived interconnection schemes under full irradiation conditions as shown in the current-voltage characteristics of Fig. 6. The peak power of the 7 × 5 array is the same for both the basic and derived interconnection schemes as shown in the power-voltage characteristics of Fig. 6.

It can be seen from the figure that all the derived schemes resulted in a similar characteristic curve at STC. However, the characteristics differ much under shaded or partial shaded conditions due to the difference in the count and location of the cross-ties [16]. The impact of partial shading on various interconnection schemes of the 7 × 5 array is assessed by the utilization factor. The ratio between the maximum power generated by the PV array and the sum of the maximum power generated by the individual PV modules is defined as the utilization factor (UF).

$$\mathrm{UF} = \frac{\text{maximum power generated by PV array}}{\text{sum of maximum power generated by individual panels}} \tag{1}$$

The basic and derived configurations are analyzed under various test shading conditions (short, narrow, long, wide, and diagonal shade patterns) that mimic the real world shading scenario and the corresponding utilization factor is depicted in Fig. 7.

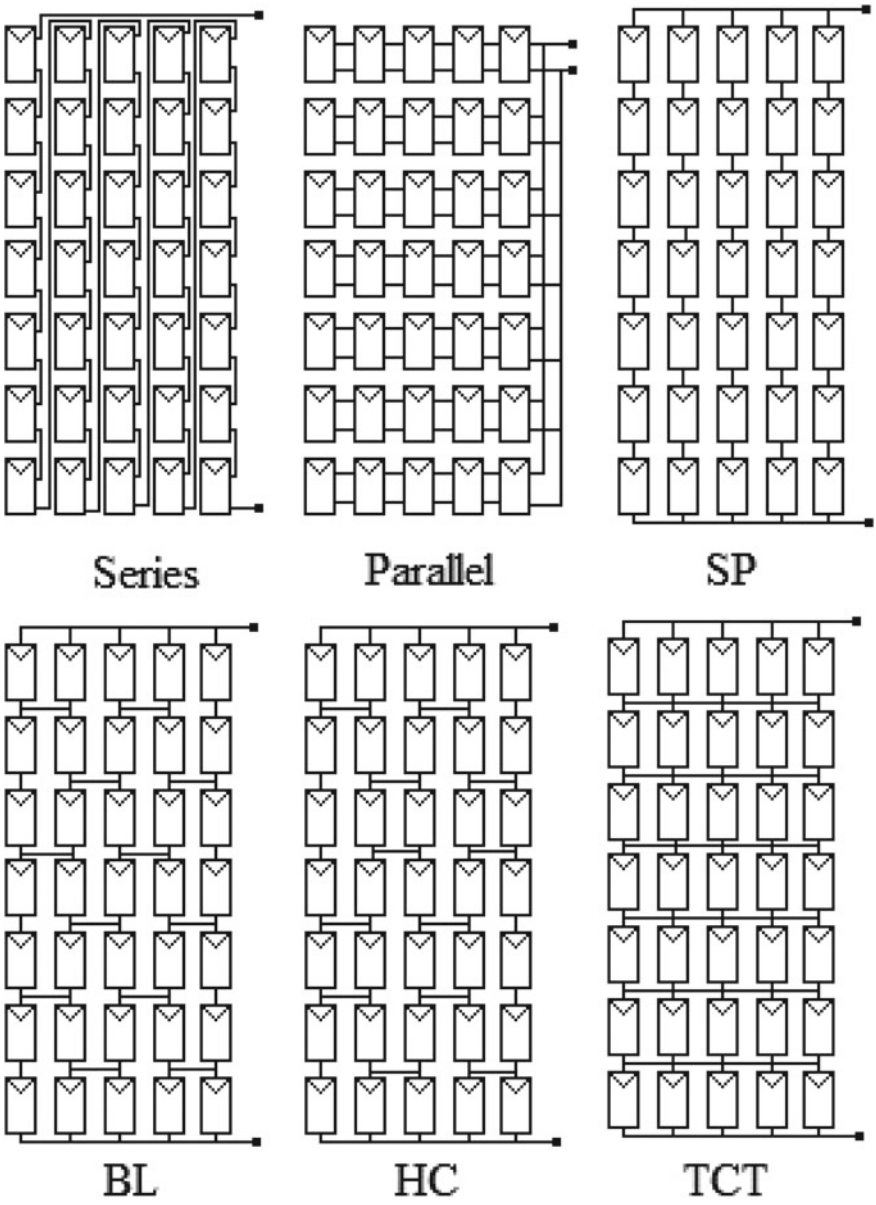

Fig. 5 Interconnection schemes of PV panels

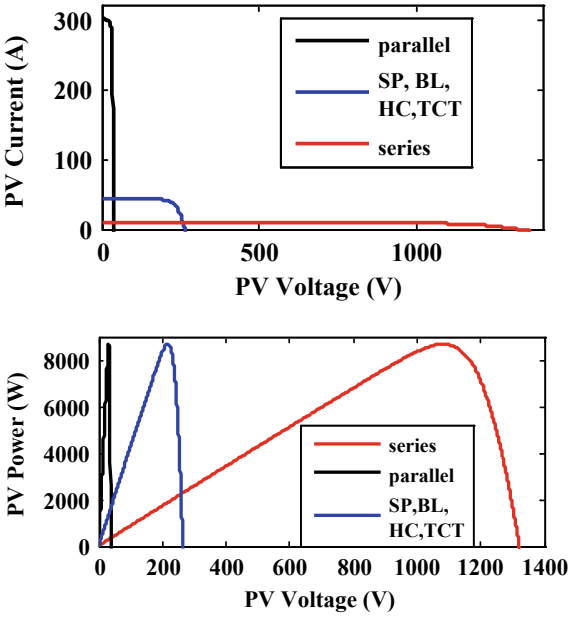

Fig. 6 Characteristics of 7 × 5 PV array under various interconnection schemes

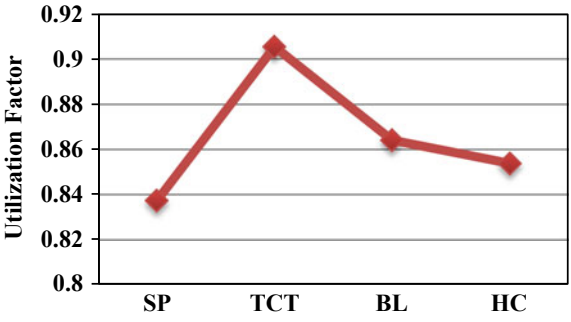

Fig. 7 Performance of interconnection schemes under various shading conditions

The presence of more cross-ties in the TCT scheme reduces the shading losses and hence it is the preferred scheme. The utilization factor can further be improved by making the PV array shade tolerant and this strategy is explained in the following section.

4 Shade Resilient PV Array (Strategy 1)

The 7 × 5 array can generate 8750 W at STC. The array is subjected to the shading pattern shown in Fig. 8 where the shade is concentrated at the corner of the array. The shade dispersion is not uniform and causes four different row currents. The first four

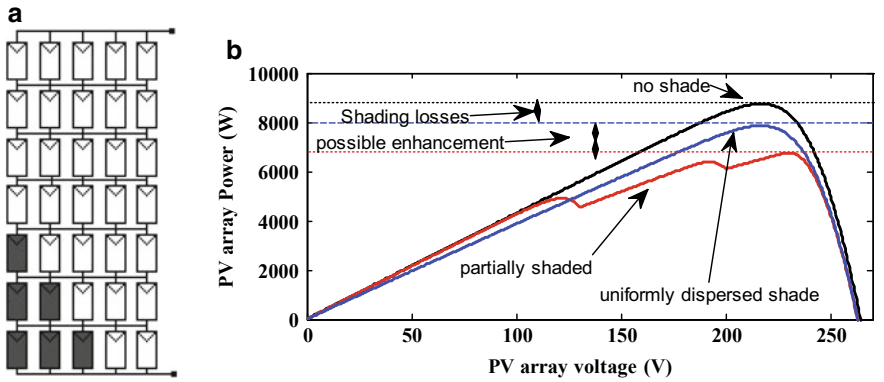

Fig. 8 **a**. Test shade pattern **b**. characteristics with and without shade dispersion

rows could generate a current of $5I_m$ (considering I_m to be the current at maximum power point). The currents generated by the fourth, fifth, and sixth rows are $4.3I_m$, $3.6I_m$, and $2.9I_m$, respectively.

The array generates a maximum power P_m of 6758 W. If the shade is uniformly dispersed all over the array, the losses due to mismatching row currents can be reduced to a greater extent. All the rows will have one shaded panel and generate a current of $4.3I_m$. The maximum generated power, in that case, will be 7853 W. Thus it is possible to enhance the power generation by dispersing the shade uniformly all over the array. This can be achieved by planning the placement of the panels within the array by shade resilient algorithm.

The arrangement of panels in a conventional TCT array is shown in Fig. 9. Each of the panels is identified by a two-digit number. The index represents the row and column numbers. For example, the index 53 points to the panel that is located in the fifth row and third column. In the conventional TCT arrangement, the panels are arranged sequentially. For example, the panels 11, 12, 13, 14, and 15 are placed next to each other in a row and are connected in parallel. The seven such paralleled strings are connected in series to form the TCT array.

The shade resilient PV array (SR PVA) places each of its panels in predetermined locations to disperse the shade uniformly all over the array. The location of the panels in the 7×5 array is determined according to the SR algorithm [17]. The SR algorithm is an offline algorithm and it uses the size of the array to calculate the displacement between the panels. The arrangement is presented in Fig. 10.

In the SR TCT arrangement, the panels that are to be physically placed in the first row are determined based on the displacement factor (DPF). The way the DPF is calculated leads to various SR arrangements [18]. One way to calculate the DPF is to divide the number of rows in the array by 2 and round it off to the floor (3 in this case).

The panel with index 11 is placed in the first row, the first column. The second panel to be physically placed next to it in the same row is determined by adding the

Fig. 9 The conventional arrangement of PV panels in 7×5 array

Fig. 10 Arrangement of panels in SR TCT

Table 2 Determination of panel location in SR TCT

Column number	Row number	Panel index
1	1	11
2	1 + 3 = 4	42
3	4 + 3 = 7	73
4	7 + 3 = 10; 10 > 7; Hence, 10−7 = 3;	34
5	3 + 4 = 6	65

DPF with the row number of the previous panel (1 + 3 = 4). This panel is to be placed in the first row, the second column, and hence the index is 42. The next panel to be placed in the first row, the third column is 73 (4 + 3 = 7). The next panel to be placed in the fourth column of the first row is 10 (7 + 3 = 10) and as 10 is greater than the array row number, 7 is subtracted from 10 (10−7 = 3). The resulting panel index is 34. The panel in the last column of the first row is 65 (3 + 3 = 6). The calculation is tabulated in Table 2.

The other rows are arranged sequentially as shown in Fig. 10. The panels 11, 12, 13, 14, and 15 are placed in different rows as highlighted and they are electrically connected in parallel. Thus, in SR arrangement, the five panels that electrically belong to a row (parallel string) are physically placed in different positions in five rows. The shade dispersion in the conventional arrangement and the SR TCT arrangement are analyzed under test shade patterns to assess the possible enhancement in power extraction.

The fixed shading is classified based on its geometry as long, short, narrow, and wide. The PV array is installed on the rooftop of residential units after careful inspection and, usually, they are shaded by parapet walls or structures on the rooftop. The most common shading pattern is short and/or narrow. The TCT and SR TCT arrays are assessed under three such fixed shading conditions.

The first shading pattern has seven shaded panels (400 W/m^2) and the shade is concentrated in four of the seven rows. The shade dispersion in conventional and SR arrangement is shown in Fig. 11a.

In the conventional arrangement, three rows are not shaded, one row has one shaded panel and three of the rows have two shaded panels each. This results in three different row currents ($5I_m$, $4.4I_m$, and $3.8I_m$) and hence the V-P curve exhibits three peaks. The maximum power that can be extracted is 7020 W as shown in Fig. 11b. The shade is dispersed in SR TCT arrangements and each of the rows has one shaded panel. The shade dispersion is uniform and each row generates a similar current (4.4 I_m). The shade dispersion and the resulting V-P curve with a single peak are shown in Fig. 11. The maximum power generated by the SR TCT array is 7671 W. The enhancement is 40 W and would be significant under heavy shading conditions.

The second shading case is shown in Fig. 12 is a short one with four shaded panels. This type of shading is commonly caused by overhead structures.

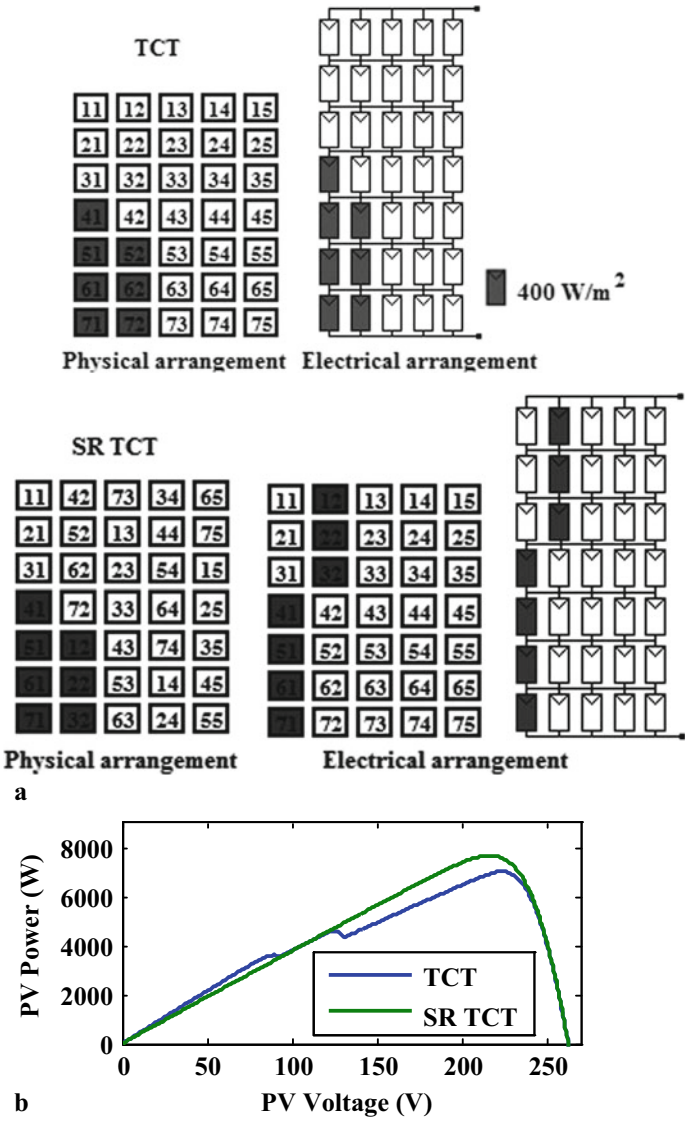

Fig. 11 Shade pattern 1 **a**. shade dispersion in TCT and SR TCT **b**. characteristics

In conventional TCT, five rows are not shaded and two rows have shaded panels. The first five rows generate a current of $5I_m$, the sixth row generates a current of $4.2I_m$ and the seventh row generates a current of $4I_m$. The three different row currents result in three peaks in the V-P curve. The maximum power generated by the conventional TCT array is 7620 W. The shade is dispersed in SR TCT and dispersion is not uniform as the shade is too short. The rows 1, 4, and 5 generate a current of $5I_m$, rows 2, 3, and

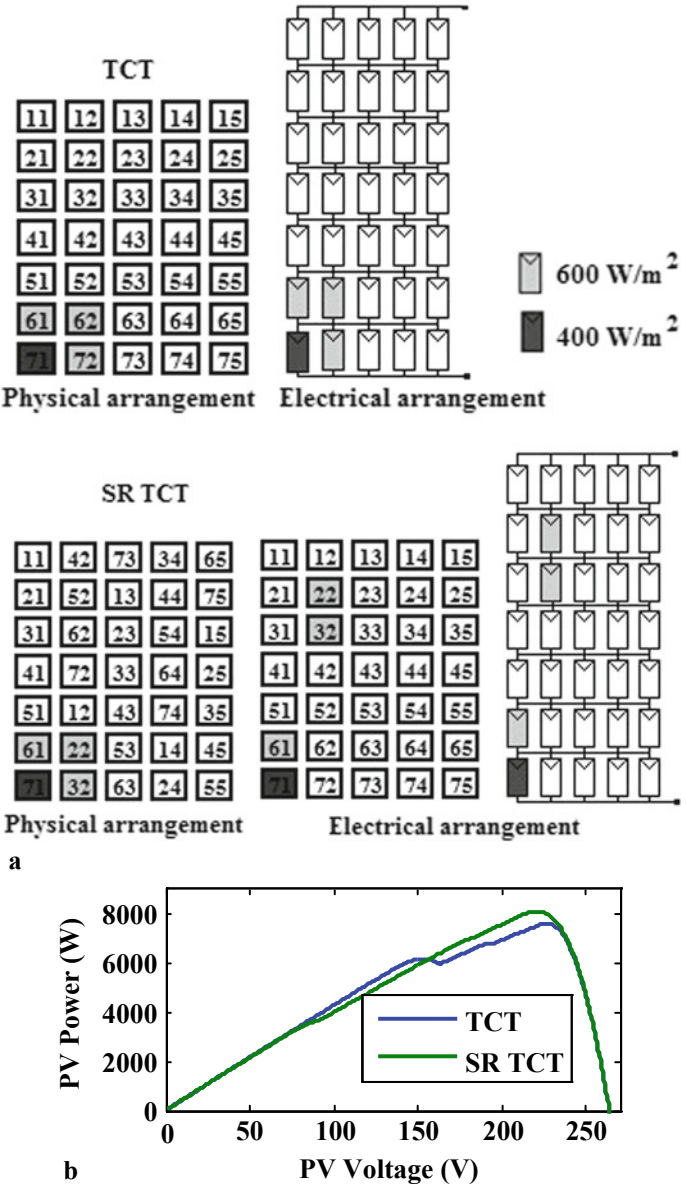

Fig. 12 Shade pattern 2 **a**. shade dispersion in TCT and SR TCT. **b**. characteristics

6 generate a current of $4.6I_m$ and the seventh row generates a current of $4.4I_m$. The V-P curve exhibits three peaks due to three different row currents. The peak power generated by the SR TCT array is 8112 W. The enhancement is significant in this case (492 W).

In the third case, all the five last row panels are shaded at 500 W/m^2 as shown in Fig. 13. This type of shade pattern is commonly caused by the parapet walls and the shading intensity remains uniform.

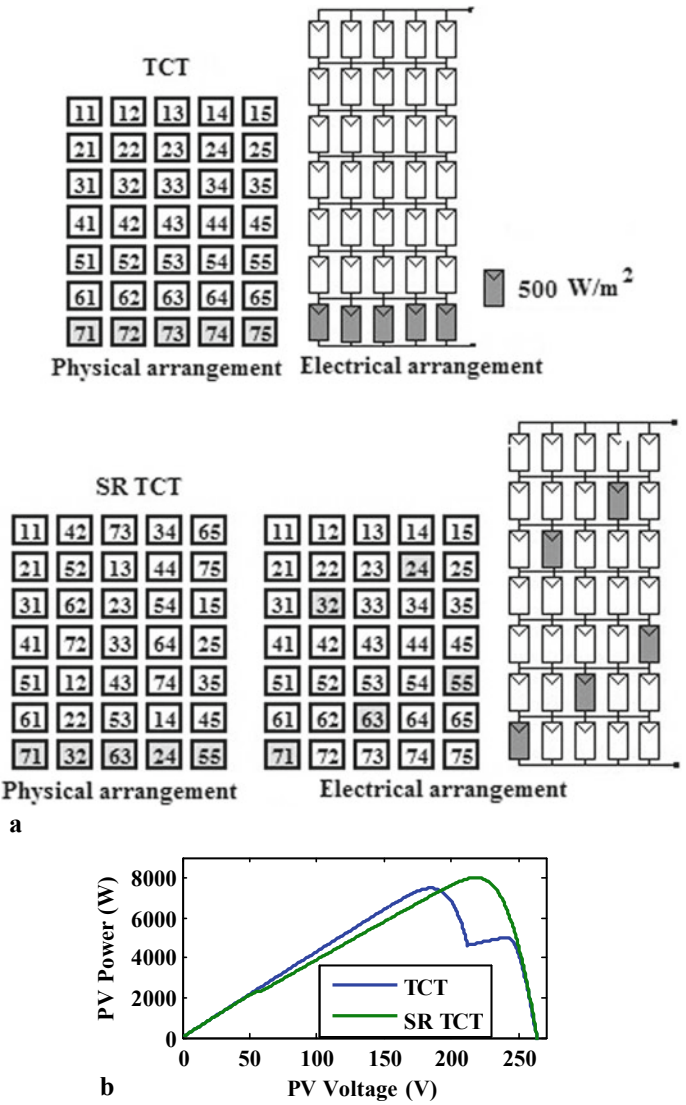

Fig. 13 Shade pattern 3 **a**. shade dispersion in TCT and SR TCT **b**. characteristics

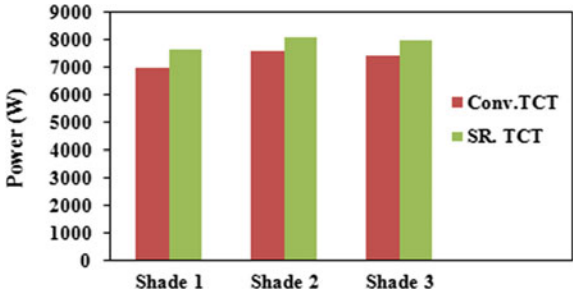

Fig. 14 Power generated by TCT and SR TCT

The conventional TCT array generates two different row currents. The first six rows generate a current of $5I_m$ and the last shaded row generates $2.5I_m$. The shaded row limits the PV array current and results in two power peaks in its V-P curve. The peak power generated by the TCT arrangement is 7468 W.

The shade is dispersed in the SR TCT arrangement as shown in Fig. 13a. Uniform shade dispersion is not possible as the shade is narrow. Five of the seven rows have one shaded panel and two rows are shade-free. Rows 1 and 4 generate a current of 5 I_m and the other rows (2, 3, 5, 6 and 7) generate a current of 4.5 I_m. The V-P curve exhibits two peaks. The peak power generated by the SR TCT is 8000 W which is significantly higher than the conventional TCT arrangement (532 W).

The peak power generated by the conventional TCT and the SR TCT arrays for the three shading conditions are compared in Fig. 14. The shade patterns considered for assessment and comparison belong to the short and narrow category as this type of shading is predominant in the residential PV system. The shade that is concentrated in a conventional arrangement is dispersed all over the array when arranged in SR TCT.

It can be inferred from Fig. 14 that the shade tolerance is better in SR TCT arrangement due to better shade dispersion. The power generation is thus enhanced under partially shaded conditions by this irradiation equivalence strategy. This is an offline strategy that does not involve switches and sensors and hence it can be adopted in residential installations without any additional cost.

This is the first strategy suggested to enhance the performance of the residential SSPV system under all environmental conditions. The SR TCT arrangement tends to disperse the shade all over the array. However, uniform dispersion is not possible if the shade is too short and/or narrow. Yet, the SR TCT arrangement enhances the output under such conditions, but multiple peaks in the V-P curve are often unavoidable. This demands the inclusion of a fast global peak detecting algorithm (GMPPT) that can discard local peaks and identify the global peak in the system.

5 Global Peak Detecting Algorithm (Strategy 2)

The commercial PV inverter has an inbuilt MPPT algorithm that can operate the PV array at its optimal power point. These algorithms are mostly conventional and cannot differentiate between the local and global peaks. The presence of multiple peaks in the V-P curve due to partial shading requires more sophisticated algorithms that can identify the global maximum.

In this study, two-line-search (golden section search and dichotomous search)-based GMPPT algorithms are analyzed and compared [19, 20]. These algorithms employ two stages. The first stage locates the region of the global peak by shrinking the search interval and the later stage identifies the global peak accurately. The first stage of both algorithms is based on the conventional fractional voltage algorithm (FVA). The fractional voltage algorithm searches for a peak at the voltage kV_{oc}. The value of k depends on environmental conditions and usually varies between 0.7 and 0.85 [21].

Partial shaded conditions are characterized by multiple peaks and hence the GMPPT algorithm has to search the entire range (0 to mV_{oc}) for the global peak. Searching each point in the search interval for the possible location of the global peak is time-consuming. To speed up the process, the first stage of the GMPPT algorithm which is based on the FVA, searches the entire search interval only at strategic voltage points (kV_{oc}, $2kV_{oc}$, $3kV_{oc}$… $7kV_{oc}$) for possible global peaks as shown in Fig. 15.

The powers at the strategic voltage points are compared and the region of the global peak is identified. The second stage of the algorithm has to locate the global peak accurately with lesser iteration by adopting 'split and remove strategy' around the region identified by the first stage. Two-line search algorithms (golden section search and dichotomous search) are assessed in this section for the 7 × 5 SR TCT array. The pseudo-codes of the two GMPPT algorithms are presented in Table 3.

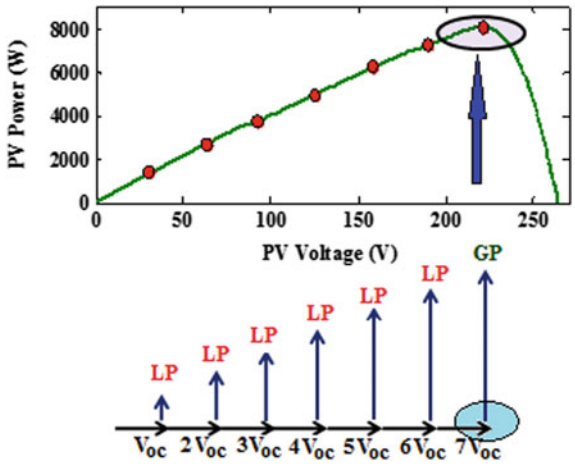

Fig. 15 First stage of GMPPT algorithm

Table 3 Pseudo-code of GMPPT algorithms

Algorithm 1 GS GMPPT	Algorithm 2 DS GMPPT
Measure PV array power and compute the change in power ΔP If $\Delta P > P_c$, initiate new tracking; P_c - critical power Stage 1 Initialize search interval (0, 7×31.5) Set $V_i = 0.83 \times 31.5$ and measure power (p_i) Apply voltage perturbation $V_{i+1} = 2 \times 0.83 \times 31.5$ and measure Power (P_{i+1}) $V_{ref-} = V_i$; if $P_i > P_{i+1}$ else $V_{ref-} = V_{i+1}$ Continue measuring power till $i = 7$;	
Stage 2 Fix search interval around V_{ref-} Fix search points $x_{1j} = b\text{-}L_j^*$ and $x_{2j} = a + L_j^*$ $L_j^* = L_o/\gamma^j$; Lo - initial search range; γ - golden ratio Measure corresponding powers P_1 and P_2 If $(P_1 - P_2) > \Delta$, If $P_1 > P_2$, discard right side section; Else discard left Fix new searching interval and probe points Measure Powers End Else GMPP located End of stage 2	Fix search interval around V_{ref-} Fix midpoint c and search points $x_1 = c\text{-}\varepsilon$, $x_2 = c + \varepsilon$; ε - tolerance value, Measure corresponding powers P_1 and P_2 If $(P_1 - P_2) > \Delta$, If $P_1 > P_2$, discard right side section; Else discard left Fix new searching interval and probe points Measure Powers End Else GMPP located End of stage 2

The GS GMPPT algorithm is based on the golden ratio and hence the name golden section search. This algorithm can detect the peak of unimodal function accurately and hence it is employed in the second stage. The initial search interval (a, b) is fixed around the region identified by the first stage. The search points x_1 and x_2 that are determined based on the golden ratio divides the search interval into three regions (a, x_1), (x_1, x_2), and (x_2, b). The corresponding powers P_1 and P_2 are measured and compared. If the power P_1 is lesser than P_2, the region (a, x_1) is rejected. The search interval is reduced from (a, b) to (x_1, b). The search continues with the new search interval as depicted in Fig. 16a and at the end of the iteration, the search interval shrinks further. The search continues until the global peak is identified.

In case of the DS GMPPT algorithm also, the search interval is fixed based on the first stage. The midpoint 'c' of the interval is fixed and the search points x_1 and x_2 are introduced on either side of 'c'. The corresponding powers P_1 and P_2 are measured and compared. If the power P_2 is greater than P_1, the region (a, x_1) is rejected. The search interval is reduced from (a, b) to (x_1, b). The search continues with the new search interval as depicted in Fig. 16b and at the end of the iteration, the search interval shrinks further. The search continues until the global peak is identified.

The second shading pattern is shown in Fig. 12 of the 7×5 array is considered to assess the performance of the two GMPPT algorithms. Both the algorithms generate the reference voltages as shown in Fig. 17 and the controller ensures accurate tracking

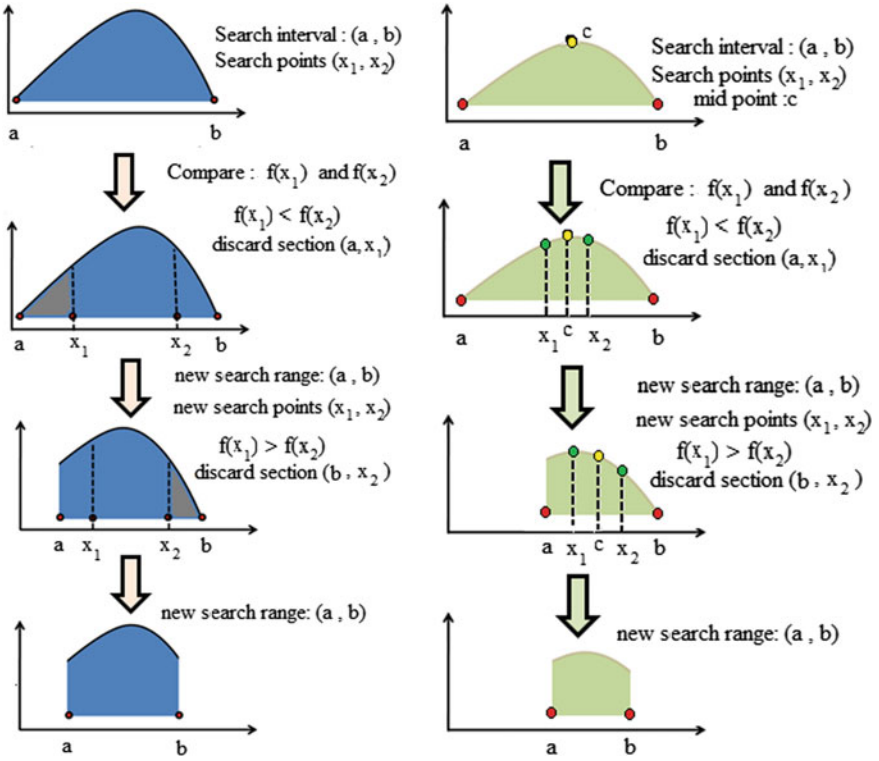

a. GS GMPPT b. DS GMPPT

Fig. 16 **a**. The second stage of the GMPPT algorithm a. GS GMPPT **b**. DS GMPPT

of the global peak. The reference voltage is compared with the actual PV array voltage. The resulting error signal is fed to the controller, which in turn adjusts the duty cycle of the power converter so as to match the source and the load impedances. When the impedances match, maximum power is extracted from the PV array.

Both the algorithms effectively tracked the global peak of 8112 W and the array is operated at 220.4 V as depicted in Fig. 17. The GMPPT algorithm waits for a significant change in power (power changes with a change in environmental or shading conditions). If the change is greater than the critical value, the algorithm initiates a new search. The first and second stages of the GMPPT algorithms then track down the global peak.

The DS GMPPT converges faster as nearly half of the search interval is discarded at the end of each of the iterations. It is quantified by a factor called the rejection ratio. The reduction ratio is defined as

$$\mathrm{RR} = \frac{L_n}{L_o} \tag{2}$$

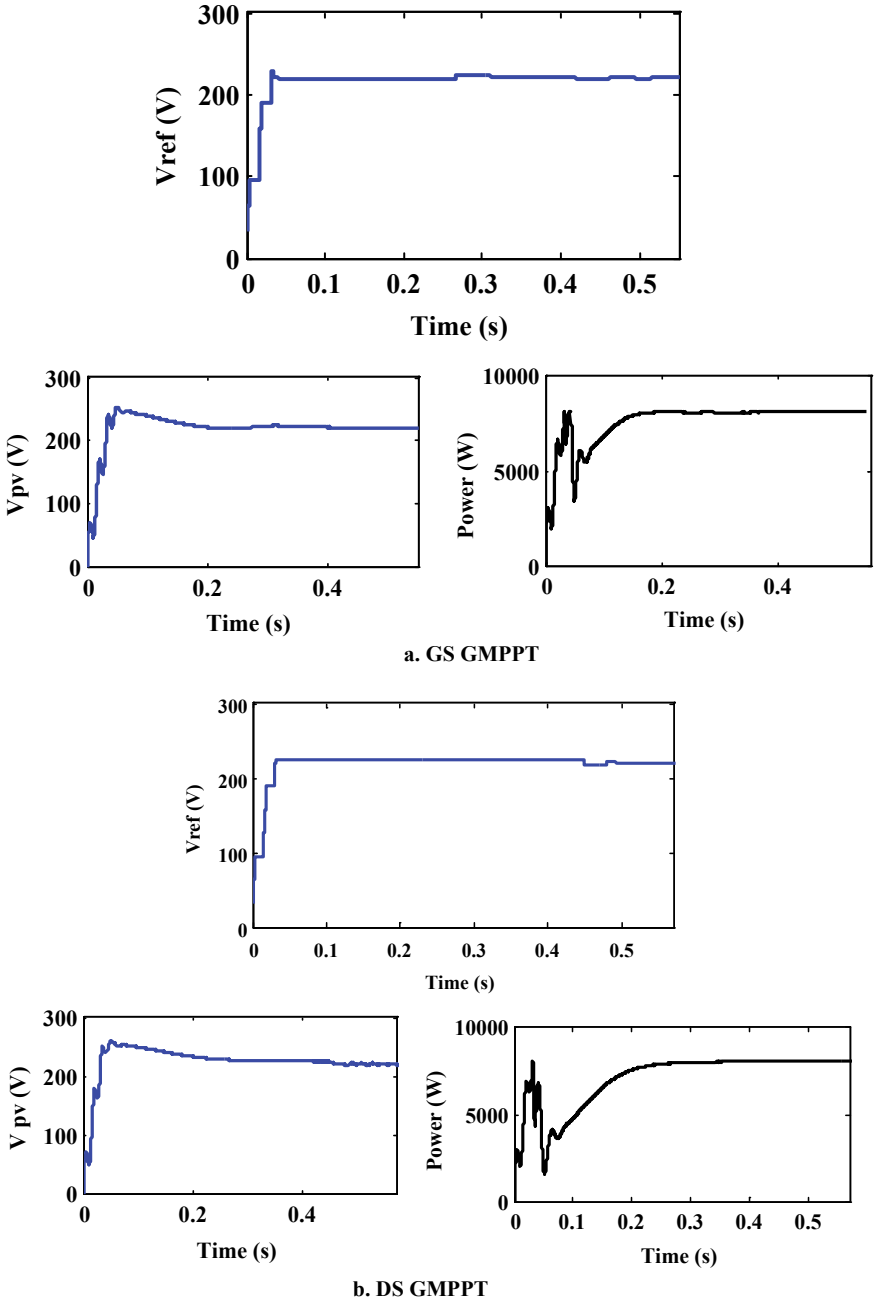

Fig. 17 Simulated results of the GMPPT algorithms **a**. GS GMPPT **b**. DS GMPPT

where L_n is the length of uncertainty after n experiments and L_o is the length of the initial interval of uncertainty. The reduction ratio of GS GMPPT is 0.618^{n-1} and that of DS GMPPT is $(2^{0.5n})^{-1}$ where n is the number of iterations. Stage one of both the algorithms locate the region of the global peak in 7 iterations. The second stage requires 14 iterations (GS GMPPT) and 12 iterations (DS GMPPT) to converge within $\pm 1\%$ of error tolerance. Hence, the DS GMPPT algorithm tracks down the global peak with 19 iterations while the GS GMPPT requires 21 iterations to converge.

Thus, with the appropriate GMPPT algorithm, the global peak of the PV array can be detected under all shading conditions and maximum power can be extracted from the 7×5 SR TCT PV array under shaded and partially shaded conditions. The extracted power is stored in a battery bank and fed to inverters to run the load in case of battery-based systems. In the case of the batteryless system, the extracted power is directly fed to the inverter.

6 Reduced Device Multilevel Inverter (Strategy 3)

The dc power extracted from the PV array is to be converted to ac to operate the utilities in the residential unit. The battery bank can be connected to the RDC MLI to convert the stored dc power to ac in the case of a battery-based system. In the batteryless system, the PV array directly feeds the MLI. The way the PV inverters are fed has led to the classification as central, string, multi-string, and micro-inverters. The central inverter has single MPPT and the output of the PV array is fed to it. If the inverter fails, the entire system shuts down. This drawback is addressed in the later developed architectures like string and multi-string structures that tend to decentralize. These structures include a dedicated MPPT for each of its strings. The provision of dedicated MPPT per string will not only improve the reliability of the system considerably but also the SSPV system's efficiency under shaded/partly shaded conditions. The arrangement is flexible and scalable as it is easy to integrate additional modules. The latest development is micro-inverters or AC Modules where the inverter is an integrated part of the PV-module. The mismatch losses and hot spot risks are totally eliminated resulting in better efficiency. The modular structure also enables easy enlargement of the system. But, the cost involved is higher than the other architectures. Generally, string/multi-string inverters are preferred over central inverters as they offer better reliability, efficiency, and scalability.

The PV inverters thus play a vital role in the PV system and often inverter failure is the major reason for the system failure. Replacing the failed inverters adds to the capital cost of the overall system and in turn, increases the return on investment period which is undesirable. It is therefore necessary to enhance the reliability of the PV inverter and in turn the reliability of the SSPV system. Reliability is assessed by counting the number of parts involved or by computing the stress on the parts. Hence, the reliability can be improved either by reducing the number of parts involved in a circuit or by reducing the stress across it.

Most of the commercial inverters adopt conventional two-level inverter or five-level inverter. The multilevel inverters have been reported as a possible solution for PV systems, with several inherent benefits, such as high efficiency, low distortion ac waveforms, and low leakage currents [22]. Additionally, in high power applications, the ac power can be synthesized from several low-level cells, i.e., low voltage semiconductors could be employed. The modular, scalable, and simpler structure of cascaded MLI (CMLI) topology makes it a preferred structure over the other conventional MLI structures like neutral point MLI and flying capacitor MLI for interfacing with the renewable sources. The major disadvantage of CMLI structure is the use of more number of semiconductor switches which reduces the reliability of the PV inverter.

Many MLI topologies that use a lesser number of switches have been proposed in the literature [23] and employing one such topology may not only improve the reliability of the inverter but also improves the spectral quality.

In this section, one such RDC MLI that has cascaded basic units and a full-bridge inverter as shown in Fig. 18 is considered. The basic unit has a dc source, a unidirectional switch, and a diode. This unit can generate one positive level $+V_1$ when the switch S_1 is closed. When the stitch is opened, the source is disconnected from the rest of the circuit. Several basic units are cascaded to generate the desired number of voltage steps at the output.

The cascaded structure is connected to a full-bridge (FB) inverter circuit to generate both positive and negative levels. The FB circuit generates a positive level if the switches T_1 and T_3 are turned on. It generates a negative level if switches T_2 and T_4 are turned on. The number of voltage levels or steps at the output is more if the inverter operates in asymmetric mode. The metrics of the RD MLI are tabulated in Table 4.

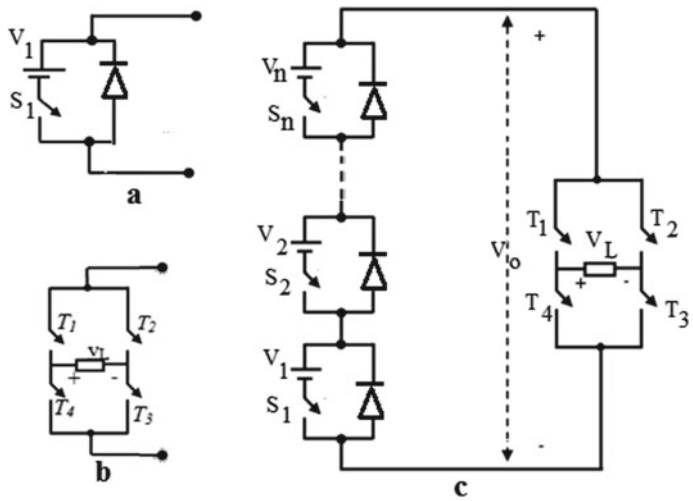

Fig. 18 RDC MLI **a**. basic unit **b**. H bridge **c**. Generalized topology

Table 4 Metrics of the RD MLI presented in Fig. 18

	RD MLI
Basic units	N
Levels generated	$2n + 1$; Symmetric mode $2^{n+1}-1$; Asymmetric mode
Switches required	$n + 4$
Voltage sources	N
Magnitudes of dc sources	V_{dc}; Symmetric mode $2^{n-1}V_{dc}$; Asymmetric mode
Maximum V_{out}	$n\ V_{dc}$; Symmetric mode $2^{n}-1V_{dc}$; Asymmetric mode
Driver circuits required	$n + 4$

The conventional CMLI can be operated in two asymmetric modes (binary and trinary) and the trinary mode generates more voltage steps at the output. Hence, the level to switch ratio is better for that mode. The RD MLI (asymmetric mode) suggested in this section is compared with that of the CMLI in the trinary mode as in Table 5.

The RD MLI can generate 31 voltage levels with 8 switches whereas; the CMLI (trinary mode) can generate only 9 levels. The level to switch ratio of the RD MLI is relatively higher than that of the CMLI in trinary mode.

A 15-level inverter with a reduced number of devices is presented in Fig. 19. It has three cascaded basic units and a FB inverter unit. The circuit uses seven switches, three sources, and three diodes. The source V_1 is connected to the FB when switch S_1 is turned on. The sources V_1 and V_2 add up and appear across the FB by switching

Table 5 Comparison of RD MLI presented in Fig. 18 and CMLI

	RD MLI (Asymmetric)	CMLI (Trinary)
Basic units	n	N
Levels generated	2^{n+1-1}	3^{n}
Switches required	$n + 4$	4n
Voltage sources required	n	n
Magnitudes of dc sources	$2^{n-1}V_{dc}$; Asymmetric mode	$3^{n-1}\ V_{dc}$
Maximum V_{out}	$2^{n}-1V_{dc}$; Asymmetric mode	$(3^{n}-1)/2\ V_{dc}$
Driver circuits required	$n + 4$	4n
Level to switch ratio	$2^{n+1-1}/n + 4$	$3^{n}/4n$

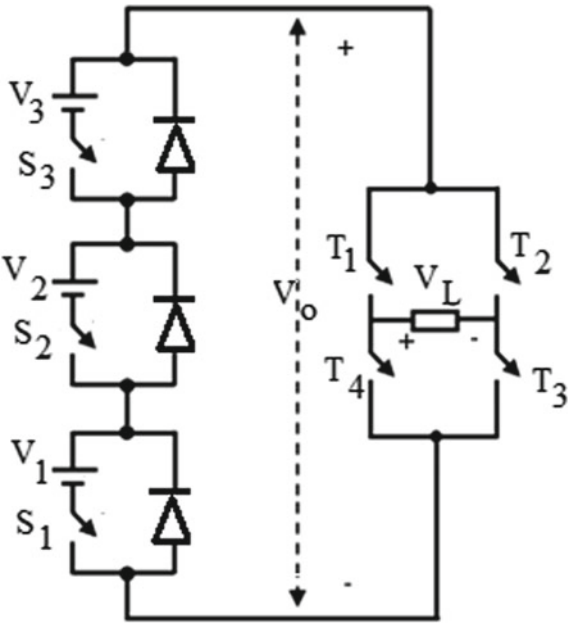

Fig. 19 15-level RD MLI

on S_1 and S_2. The voltage across the load is positive if switches T_1 and T_3 are turned on and it is negative if the other two switches are turned on.

The magnitudes of the dc sources are chosen to be V_{dc}, $2V_{dc,}$ and $4V_{dc}$. Capacitors can also be used to split the voltage from the source. The required gating pulses are generated by a fundamental frequency modulation strategy called half-height PWM scheme [24] which determines the instant at which the switches are to be triggered. The switches are triggered sequentially as presented in Table 6.

The simulated output voltage [25] and the harmonic profile of the 15-level RD MLI are presented in Fig. 20. The output voltage waveform shows 15 distinct voltage steps and the % THD is found to be 1.88% without using filters. The Spectral quality improves with the number of voltage steps. The more the number of levels, the more the output waveform gets closer to the sine wave. But, the number of switches and the allied circuit increases with the levels and it, in turn, will affect the reliability of the inverter due to increased part count. The 15-level RD MLI presented in Fig. 19 has produced a stepped voltage waveform with a lesser harmonic distortion (1.88%) that is within the desirable limits. Hence, it is not required to extend the number of levels further compromising reliability.

The conventional cascaded MLI can generate 15 voltage levels when operated in binary mode. The CMLI cannot generate 15 levels in trinary mode. Hence, the metrics of the RD MLI presented in Fig. 19 are compared with CMLI (binary mode) in Table 7.

The 15-level RD MLI has used only 7 switches as compared to 12 in conventional CMLI (Binary) to generate 15 unique voltage steps at the output. The %THD (1.88%)

Table 6 Status of switches and the output voltage

States	Status of switches							Output Voltage
	S_1	S_2	S_3	T_1	T_2	T_3	T_4	
1				✓	✓			0
2	✓			✓		✓		V_{dc}
3		✓		✓		✓		$2V_{dc}$
4	✓	✓		✓		✓		$3V_{dc}$
5			✓	✓		✓		$4V_{dc}$
6	✓		✓	✓		✓		$5V_{dc}$
7		✓✓	✓	✓		✓		$6V_{dc}$
8	✓	✓	✓	✓		✓		$7V_{dc}$
9	✓✓				✓		✓	$-V_{dc}$
10		✓			✓		✓	$-2V_{dc}$
11	✓	✓			✓		✓	$-3V_{dc}$
12			✓		✓		✓	$-4V_{dc}$
13	✓		✓		✓		✓	$-5V_{dc}$
14		✓	✓		✓		✓	$-6V_{dc}$
15	✓	✓	✓		✓		✓	$-7V_{dc}$

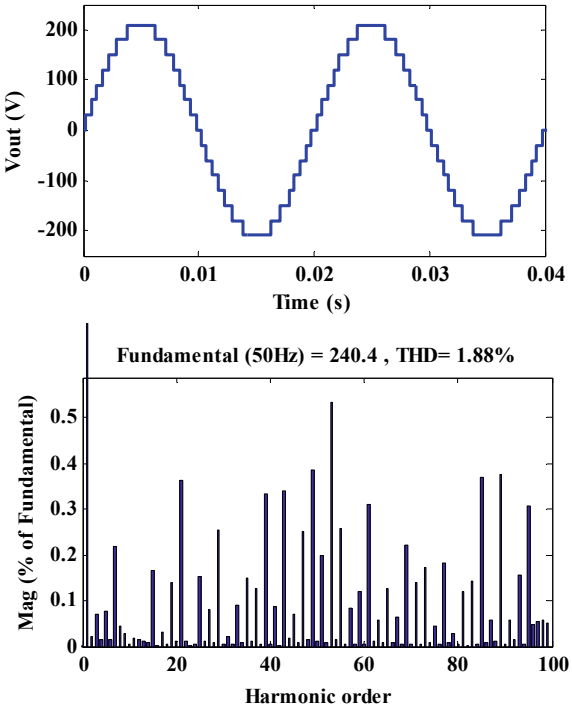

Fig. 20 Simulated output and harmonic profile of the 15-level RD MLI

Table 7 Comparison between CMLI (B) and RD MLI in Fig. 19

	CMLI (Binary)	RD MLI
Number of levels	15	15
Number of switches	12	7
Number of dc sources	3	3
Magnitudes of dc sources	V_{dc}, $2V_{dc}$, 4 V_{dc}	V_{dc}, $2V_{dc}$, 4 V_{dc}
Maximum V_{out}	7 V_{dc}	7 V_{dc}
Number of gate driver circuits	12	7
Level to switch ratio	1.25	2.14

is also well within the desirable limits. The reduction in the switches involved reduces the driver circuit requirements and it in turn reduces the overall part count. Reliability can be assessed based on the number of components involved. As this RD MLI adopts fewer components than the conventional topology, the reliability is much better. Further, the number of switches that are turned on at any given instant is less compared to the conventional topologies and hence the losses involved are also reduced.

Thus, the performance of the SSPV system can be improved by incorporating all three enhancement strategies, SR TCT, GMPPT, and RD MLI along with the standard design procedure. The enhanced SSPV system is depicted in Fig. 21.

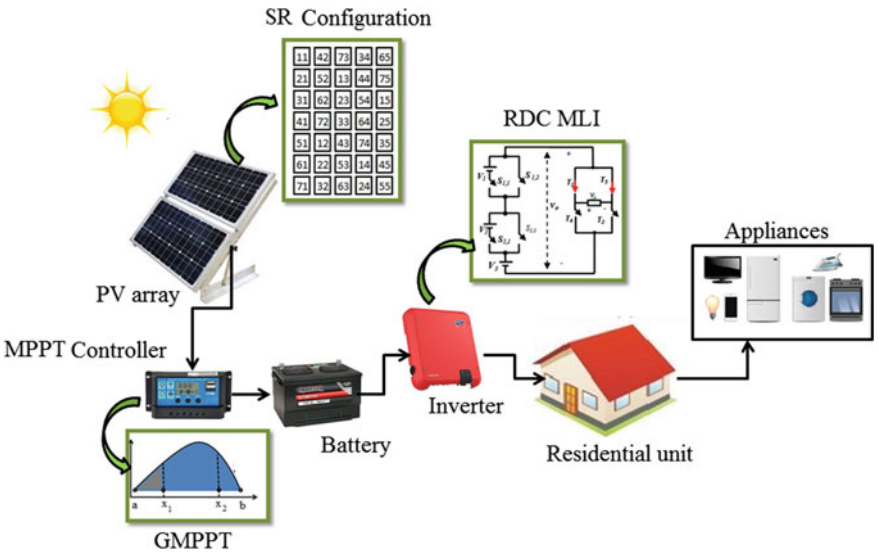

Fig. 21 Enhanced SSPV system

The power extracted from the PV array can be enhanced by improving equalizing the irradiation received by the panels. This is achieved by arranging the panels according to the SR algorithm and adopting TCT interconnection. This arrangement enhances the output under all environmental conditions by minimizing the mismatch losses due to shading/partial shading. Incorporating a fast and accurate GMPPT algorithm operates the PV array at its optimal point and ensures the transfer of maximum power from the source to the load. The reliability of the inverter and in turn the SSPV system can be improved by employing RD MLI.

7 Conclusion

This chapter has elaborately explained the impact of partial shading on the performance of the PV array and has suggested three strategies to improve the power generation under such conditions. The SSPV system is designed for a residential unit using standard procedures and the suggested strategies are demonstrated in the design. The role of interconnection schemes of a partially shaded PV array is assessed in terms of UF and it is suggested that the TCT scheme is a better option. Further, shade resilience is included in the TCT PV array by adopting the irradiation equivalence strategy. The panels are arranged according to an offline algorithm in SR TCT array and this arrangement tends to disperse the shade evenly among the rows. The mismatch in row currents is thus reduced and the power generation is enhanced without additional cost. This strategy is best suited for small residential installations. Shade dispersion may not be uniform if the shade is short and narrow as in most of the practical cases and results in multiple peaks in the V-P curve. Many algorithms are reported in the literature and the selection depends on the requirements and the availability of resources. This chapter has suggested two-line-search-based GMPPT algorithms (GSS and DS) that can detect the global peak accurately and quickly. The DS GMPPT algorithm is faster compared to the GSS algorithm as the search interval is almost reduced to half at the end of each of the iterations. RD MLI is suggested as the third strategy to improve the reliability of the system. Reduced device count improves reliability, as the part count is reduced. A 15-level inverter is developed based on the suggested topology and its working is explained in detail. Many new topologies are reported in the literature and appropriate structure can be selected based on the requirements and size of the PV array and/or battery bank. All three suggested strategies can be considered while designing an SSPV system to enhance its performance under all environmental conditions.

References

1. Ibrahim H, Anani N (2020) A Study of the effect of different configurations of bypass diodes on the performance of a PV string. Sustainability in energy and buildings, pp 593–600
2. Motamarri R, Nagu B (2020) GMPPT by using PSO based on Lévy flight for photovoltaic system under partial shading conditions. IET Renew Power Gener 14(7):1143–1155
3. Nguyen BN, Nguyen VT, Duong MQ, Le KH, Nguyen HH, Doan AT (2020) Propose a MPPT algorithm based on Thevenin equivalent circuit for improving photovoltaic system operation. Front Energy Res 8:14
4. Zou Y, Yan F, Wang X, Zhang J (2020) An efficient fuzzy logic control algorithm for photovoltaic maximum power point tracking under partial shading condition. J Franklin Inst 357(6):3135–3149
5. Eltamaly AM (2015) Performance of smart maximum power point tracker under partial shading conditions of PV systems. In: 2015 IEEE International conference on smart energy grid engineering (SEGE). IEEE
6. Ajmal AM, Babu TS, Ramachandaramurthy VK, Yousri D, Ekanayake JB (2020) Static and dynamic reconfiguration approaches for mitigation of partial shading influence in photovoltaic arrays. Sustain Energy Technol Assess 40:100738
7. Sagar G, Pathak D, Gaur P, Jain V (2020) A Su Do Ku puzzle based shade dispersion for maximum power enhancement of partially shaded hybrid bridge-link-total-cross-tied PV array. Solar Energy 204:161–180
8. El Iysaouy L, Lahbabi M, Baskys A, Oumnad A (2020) Performance analysis of partially shaded photovoltaic array using magic square view configuration for shade dispersion. J Solar Energy Eng 142(6)
9. Yadav AS, Mukherjee V (2018) Line losses reduction techniques in puzzled PV array configuration under different shading conditions. Solar Energy 171:77–783
10. Farh HMH, Eltamaly AM, Othman MF (2018) Hybrid PSO-FLC for dynamic global peak extraction of the partially shaded photovoltaic system. PloS one 13(11): e0206171
11. Akrami M, Pourhossein K (2018) A novel reconfiguration procedure to extract maximum power from partially-shaded photovoltaic arrays. Solar Energy 173:110–119
12. Schettino G, Pellitteri F, Ala G, Miceli R, Romano P, Viola F (2020) Dynamic reconfiguration systems for PV plant: Technical and economic analysis. Energies 13(8)
13. https://solargis.com/maps-and-gis-data/download/india
14. Walker L, Hofer J, Schlueter A (2019) High-resolution, parametric BIPV and electrical systems modeling and design. Appl Energy 238:164–179
15. Sahoo SK, Shah M, Dawlatzai NA, Amalorpavaraj RAJ (2020) Assessment of mismatching in series and parallel connection of the PV modules of different technologies and electrical parameters. In 2020 International conference on computer communication and informatics, pp 1–5
16. Malathy S, Ramaprabha R (2015) Comprehensive analysis on the role of array size and configuration on energy yield of photovoltaic systems under shaded conditions. Renew Sustain Energy Rev 49:672–679
17. Malathy S, Ramaprabha R (2020) Shade resilient total cross tied configurations to enhance energy yield of photovoltaic array under partial shaded conditions. Emerg Trends Comput Expert Technol 35:122–133. Springer
18. Malathy S, Ramaprabha R (2018) Reconfiguration strategies to extract maximum power from photovoltaic array under partially shaded conditions. Renew Sustain Energy Rev 81:2922–2934
19. Mostafa HH, Ibrahim AM, Anis WR (2019) A performance analysis of a hybrid golden section search methodology and a nature-inspired algorithm for MPPT in a solar PV system. Arch Electr Eng 611–627
20. Malathy S, Ramaprabha R (2020) Tracking the maximum power point of PV array using dichotomous search. U.P.B. Sci Bull Ser C82(1):179–188
21. Baimel D, Tapuchi S, Levron Y, Belikov J (2019) Improved fractional open circuit voltage MPPT methods for PV systems. Electronics 8(3):321

22. Kumar N, Saha TK, Dey J (2020) Multilevel inverter (MLI)-based stand-alone photovoltaic system: modeling, analysis, and control. IEEE Syst J 14(1):909–915
23. Salem A, Robbersmyr KG, Norambuena M, Rodriguez J (2020) Voltage source multilevel inverters with reduced device count: topological review and novel comparative factor. IEEE Trans Power Electron
24. Malathy S, Ramaprabha R (2019) Reliability and performance assessment of reduced component count multilevel inverter for PV systems. AIP Conf Proc 2161:020017
25. www.mathworks.com